

Supplementary Information

Explicit analysis of functional-group orientation in amorphous organic semiconductor films by using deuterated materials

*Yoshihito Sukegawa, Yuro Yagi, Hideyoshi Kitahara, Shunji Mochizuki, Daisuke Yokoyama**

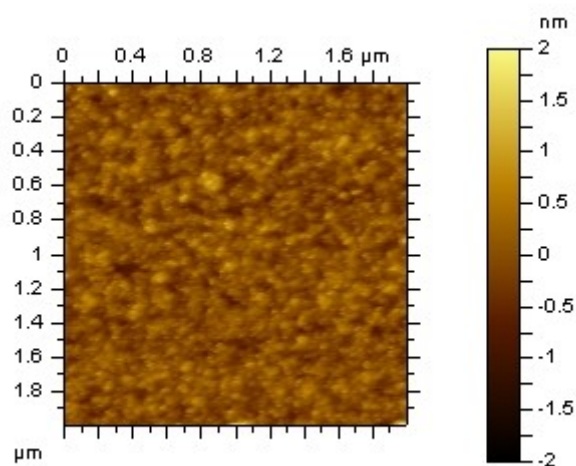


Fig. S1 AFM image of a 100-nm-thick BPBPA-D0 film deposited on a Si(100) substrate. The RMS value of the surface roughness is 0.27 nm.

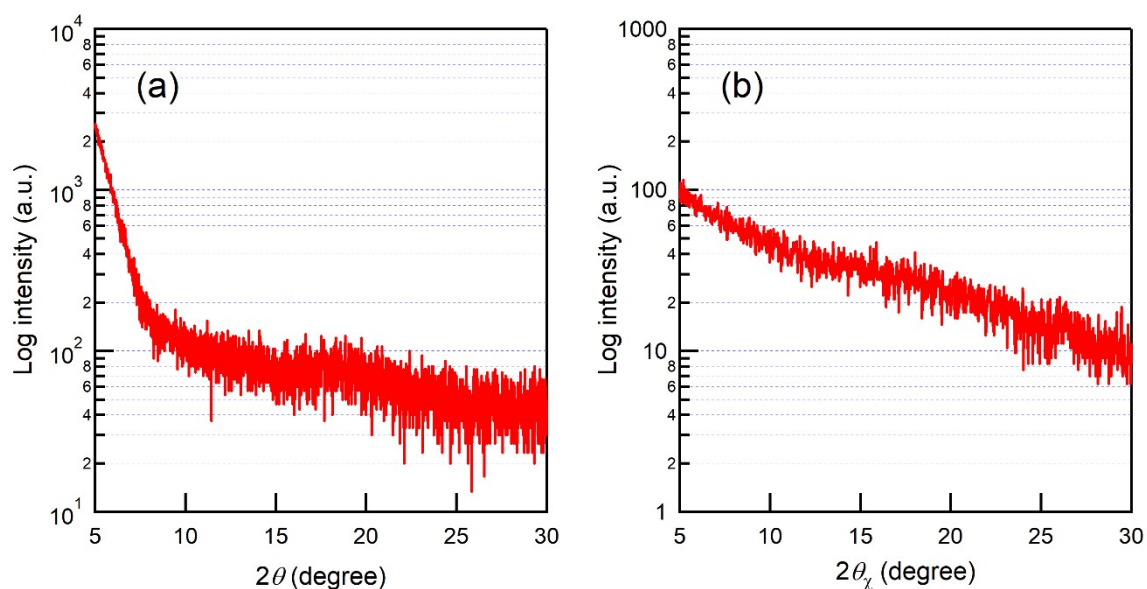


Fig. S2 (a) Out-of-plane and (b) in-plane XRD patterns of a 100-nm-thick BPBPA-D0 film deposited on a Si(100) substrate.

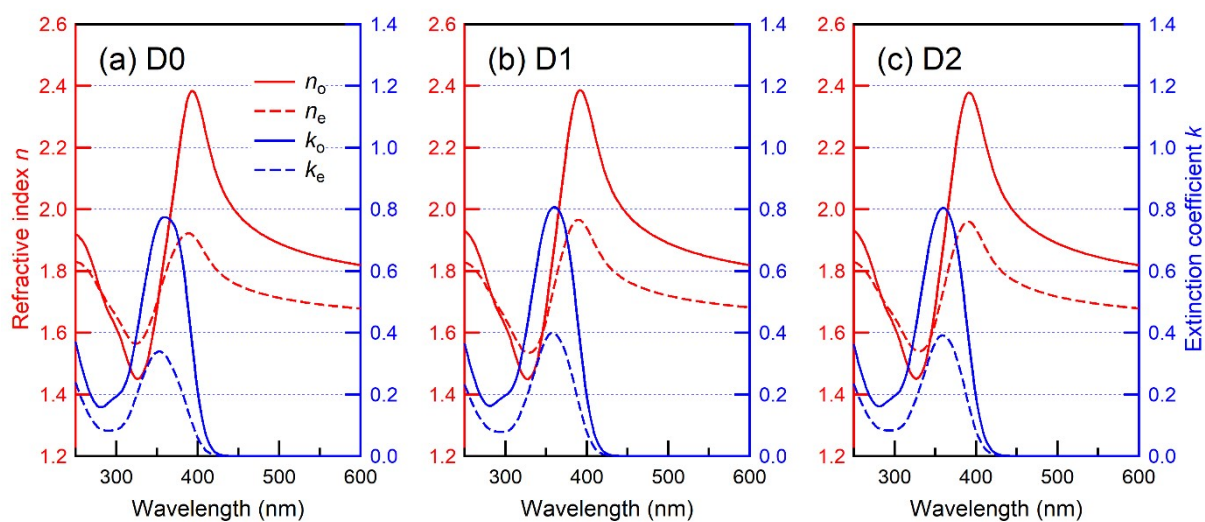


Fig. S3 Anisotropic refractive indices and extinction coefficients of 100-nm-thick as-deposited films of (a) BPBPA-D0, (b) D1, and (c) D2 determined by VASE.

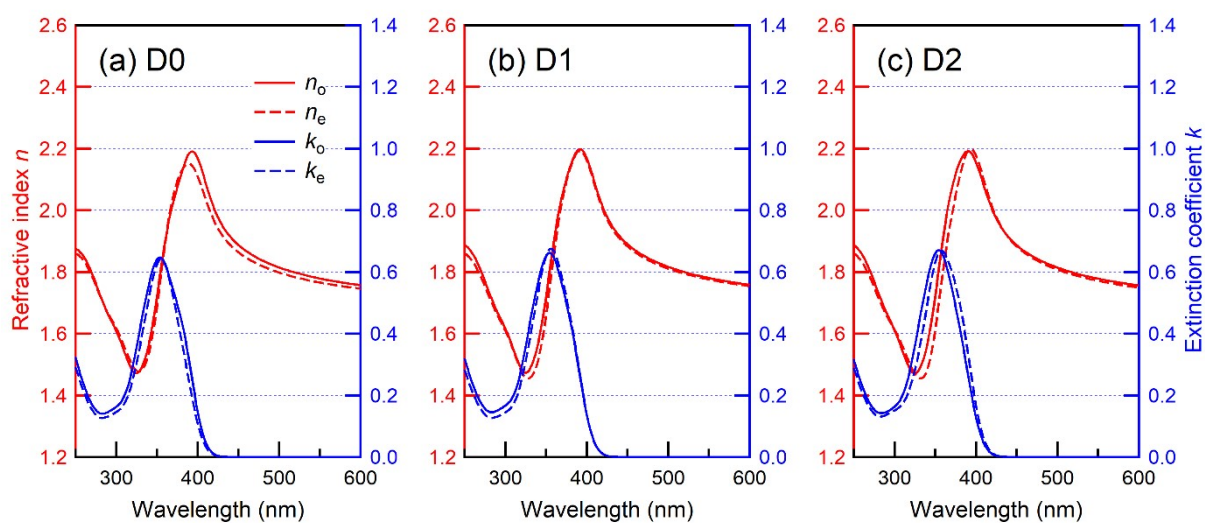


Fig. S4 Anisotropic refractive indices and extinction coefficients of 100-nm-thick annealed films of (a) BPBPA-D0, (b) D1, and (c) D2 determined by VASE.

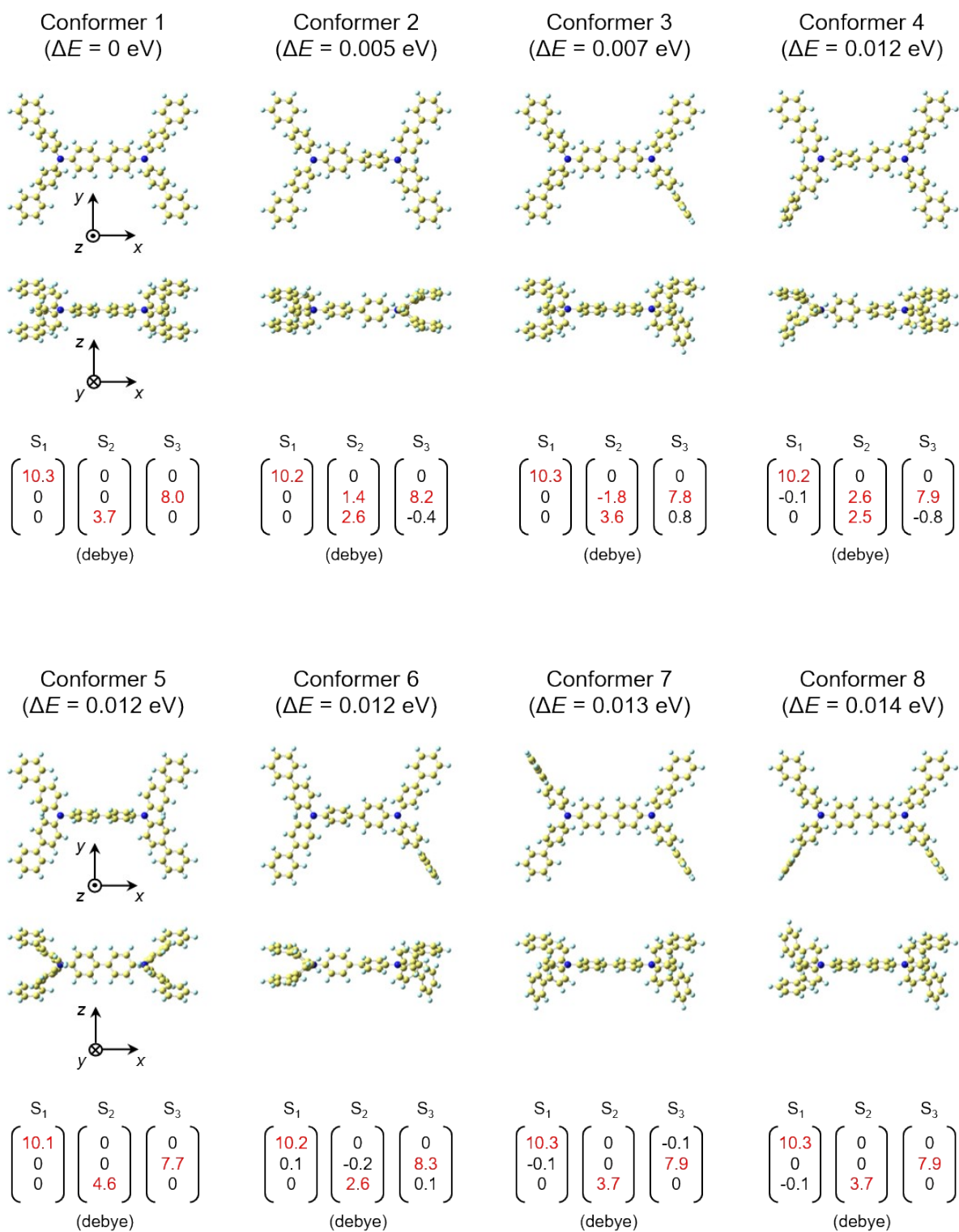


Fig. S5 Steric structures and transition dipole moment vectors for low-energy electronic transitions of the 24 conformers of BPBPA molecules. The differences in the steric energy are also shown as ΔE .

(Continued on next page)

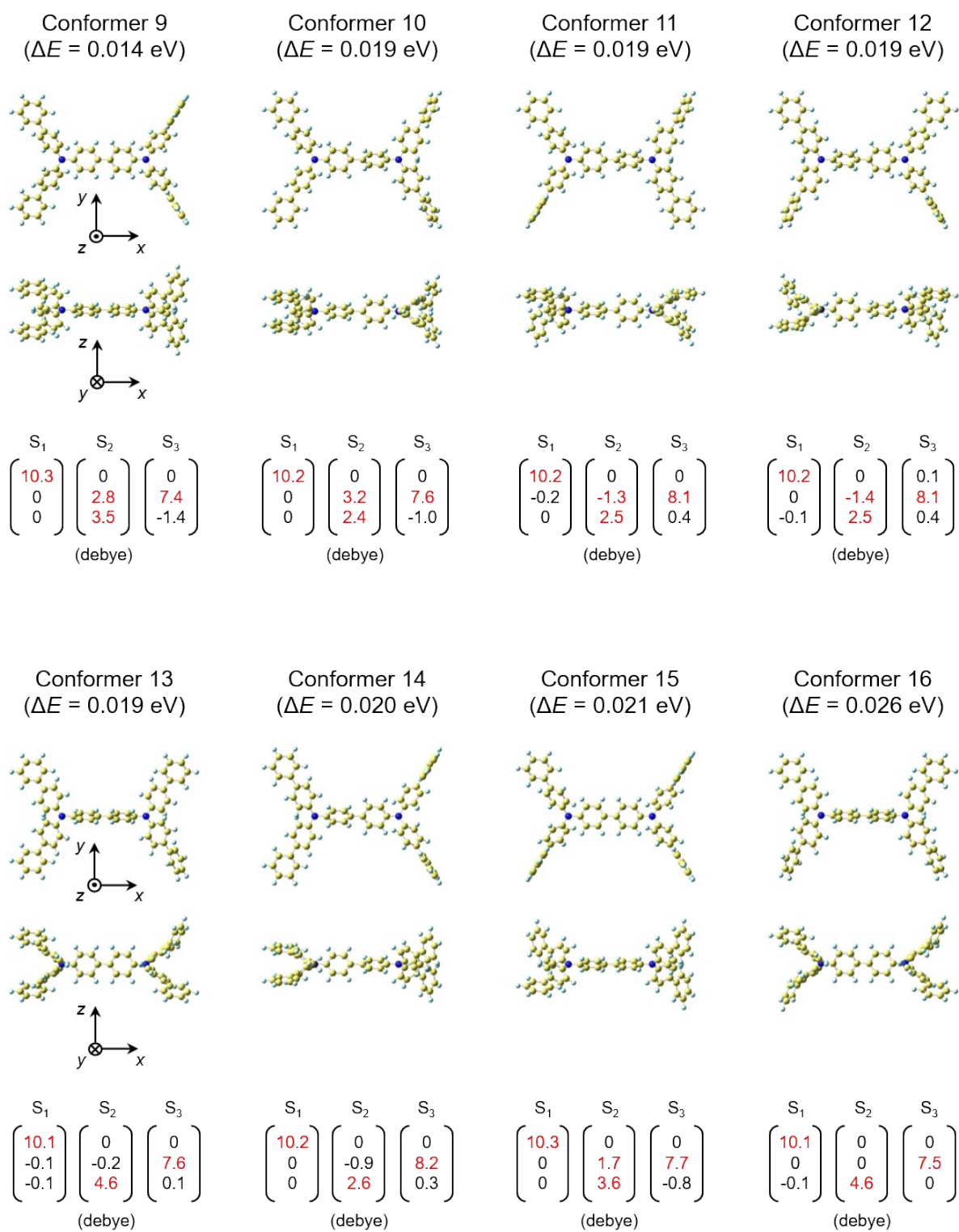


Fig. S5
(Continued from the previous page)

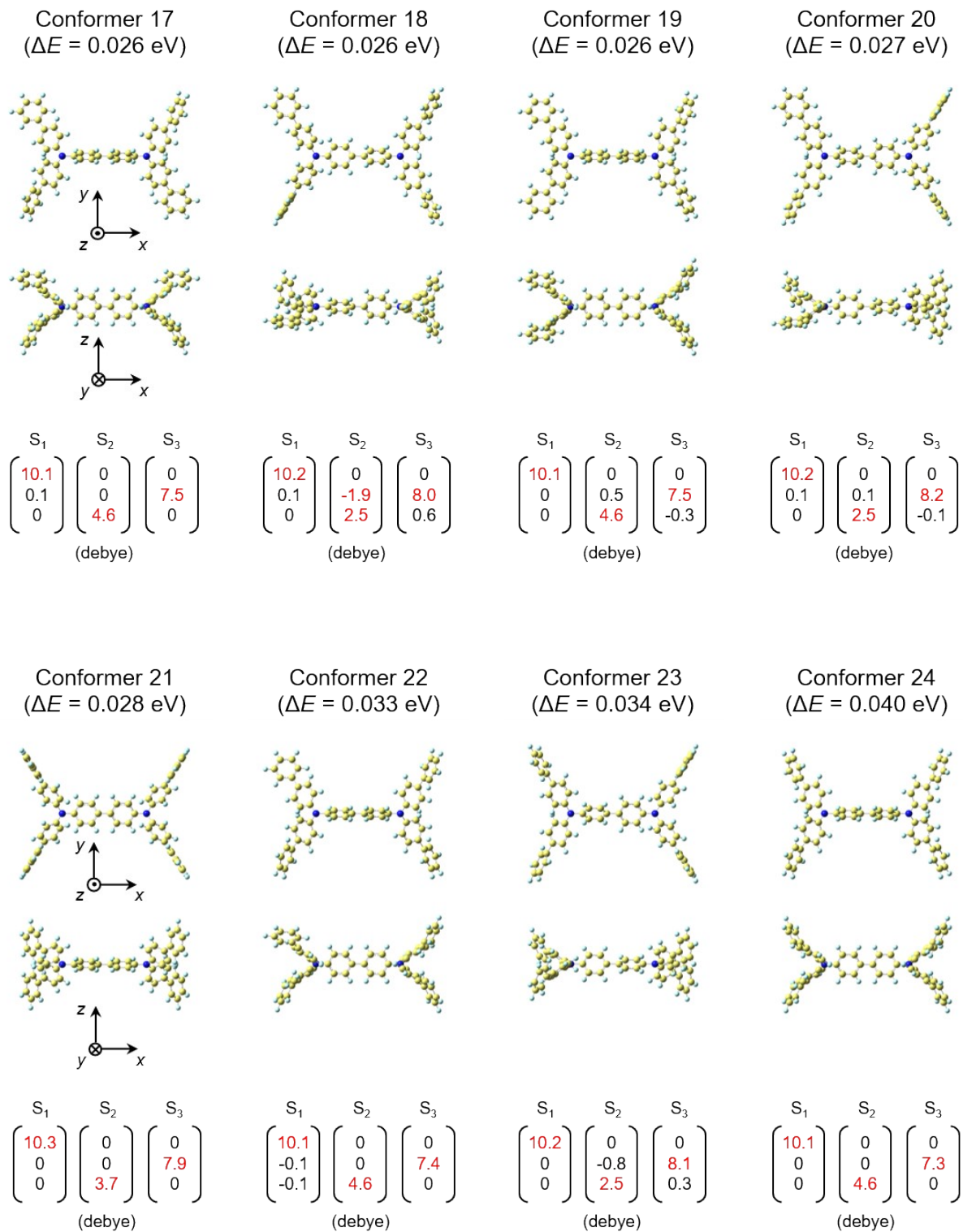
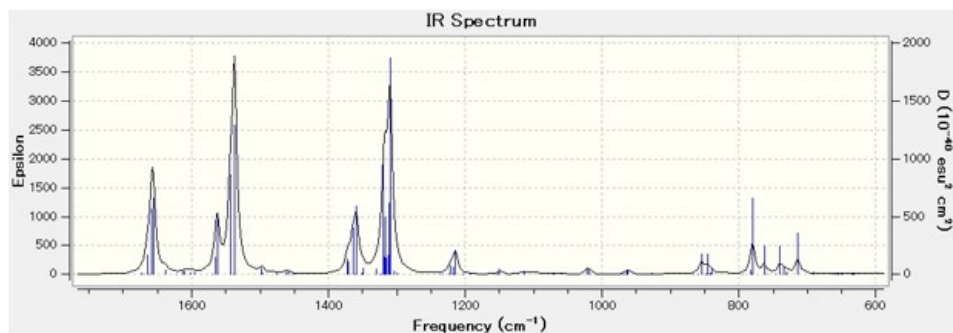
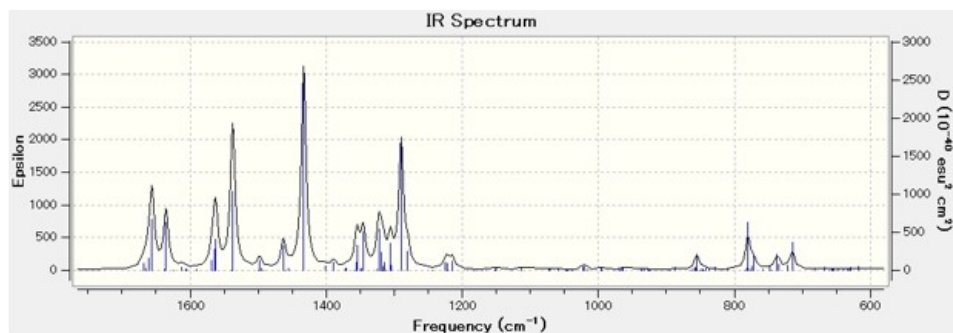


Fig. S5
(Continued from the previous page)

(a) D0



(b) D1



(c) D2

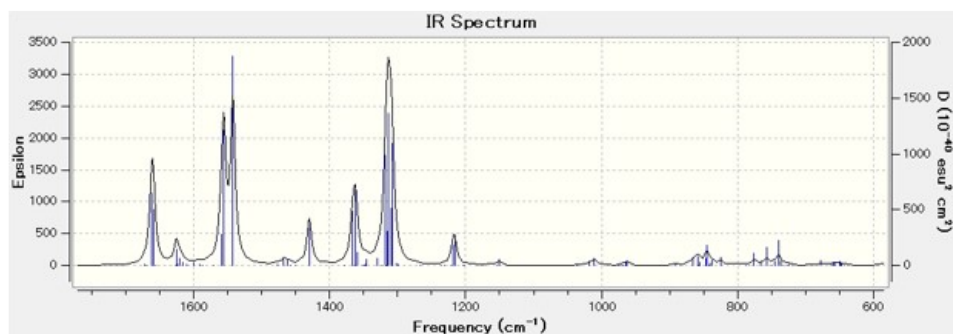


Fig. S6 Simulated IR absorption spectra of (a) BPBPA-D0, (b) D1, and (c) D2 molecules obtained by DFT B3LYP/6-31G(d) calculations.

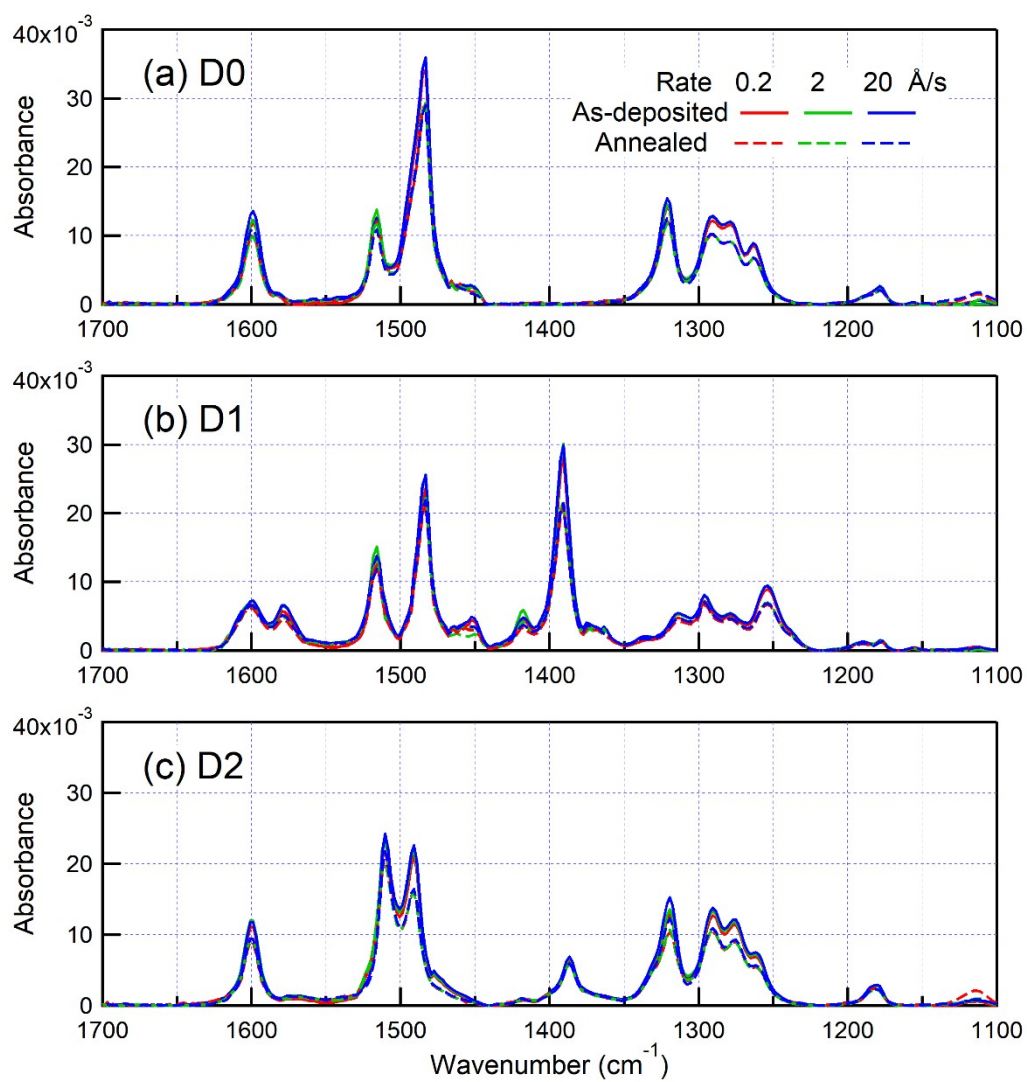


Fig. S7 Dependence of IR absorption spectra of 100-nm-thick as-deposited and annealed (a) BPBPA-D0, (b) D1, and (c) D2 films on the deposition rate in the spectral range of 1100–1700 cm^{-1} .

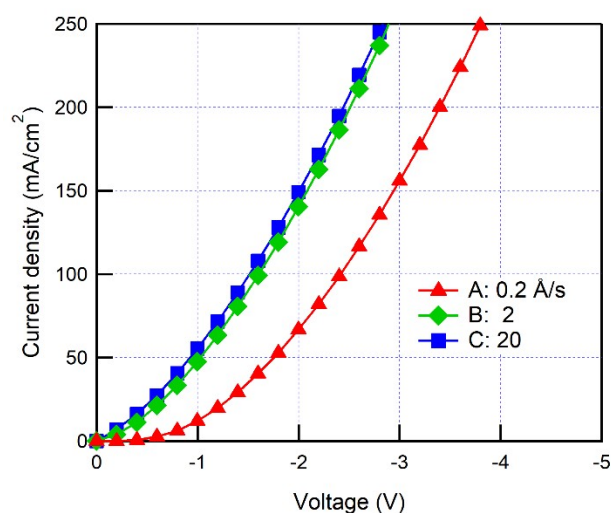


Fig. S8 J - V characteristics for negative voltage side of three hole-only devices A, B, and C, where BPBPA-D0 is deposited at three different deposition rates of 0.2, 2, and 20 \AA s^{-1} , respectively; Device A, B, and C: glass/ITO (75 nm)/HAT-CN (5 nm)/BPBPA-D0 (100 nm at 0.2, 2, and 20 \AA s^{-1})/HAT-CN (5 nm)/Au (50 nm).

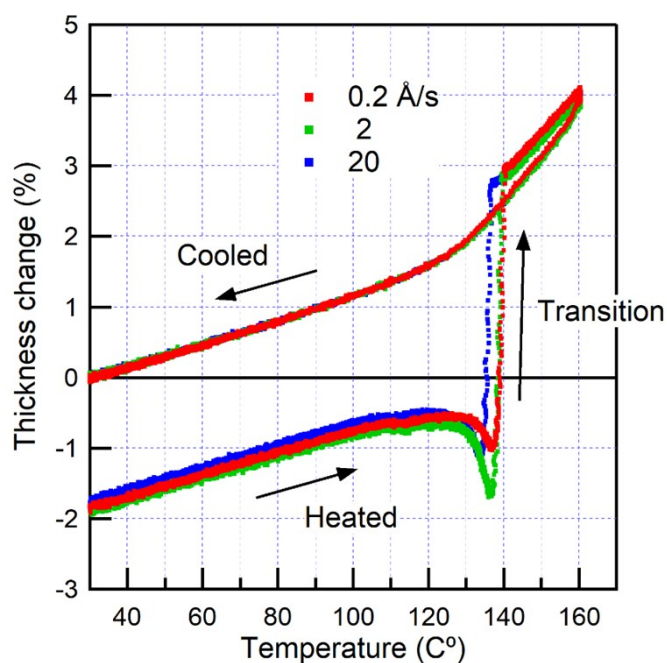


Fig. S9 Thickness changes of as-deposited BPBPA-D0 films fabricated at deposition rates of 0.2, 2, and 20 \AA s^{-1} determined by *in situ* ellipsometry during a heating-cooling cycle. To compare the relative film densities of the as-deposited films, the thicknesses at 30 $^{\circ}\text{C}$ after cooling were used as the standards for normalization. The thicknesses of the as-deposited films are $\sim 2\%$ smaller than those of the films after cooling, but there was not a substantial difference ($<0.1\%$) in the thickness of the as-deposited films fabricated at the different deposition rates.

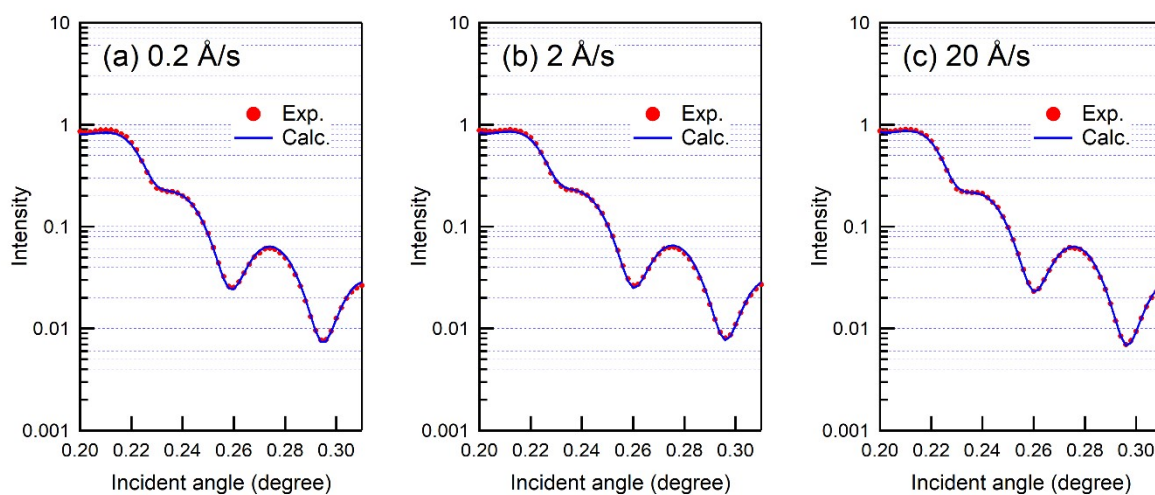


Fig. S10 XRR patterns of BPBPA-D0 films deposited on a Si(100) substrate at deposition rates of (a) 0.2, (b) 2, and (c) 20 Å s⁻¹. The analytical results of the thickness and film density are (a) 98.6 nm and 1.135 g/cm³, (b) 98.7 nm and 1.133 g/cm³, and (c) 97.9 nm and 1.138 g cm⁻³.

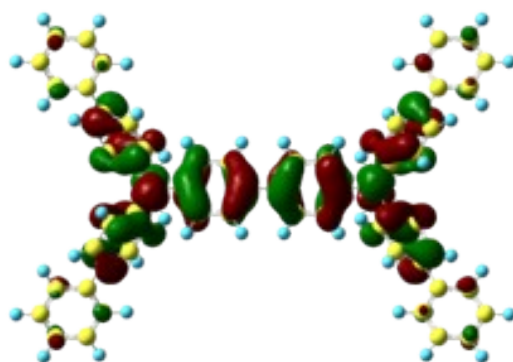


Fig. S11 Distribution of the HOMO of the BPBPA molecule obtained by DFT B3LYP/6-31G(d) calculation.

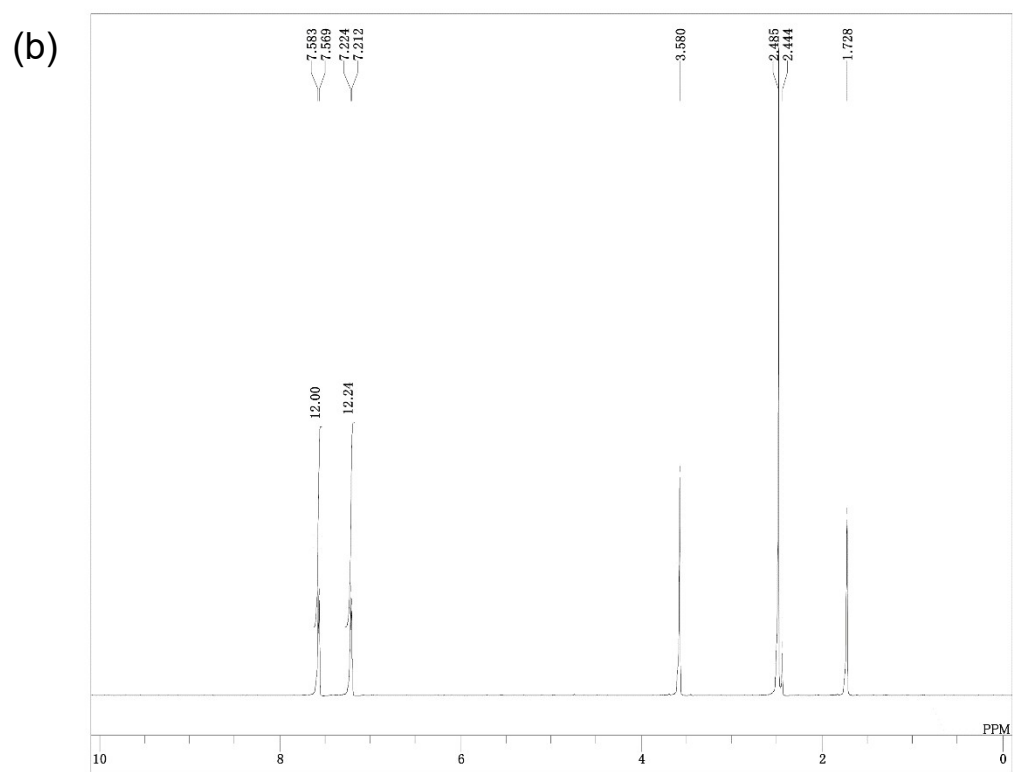
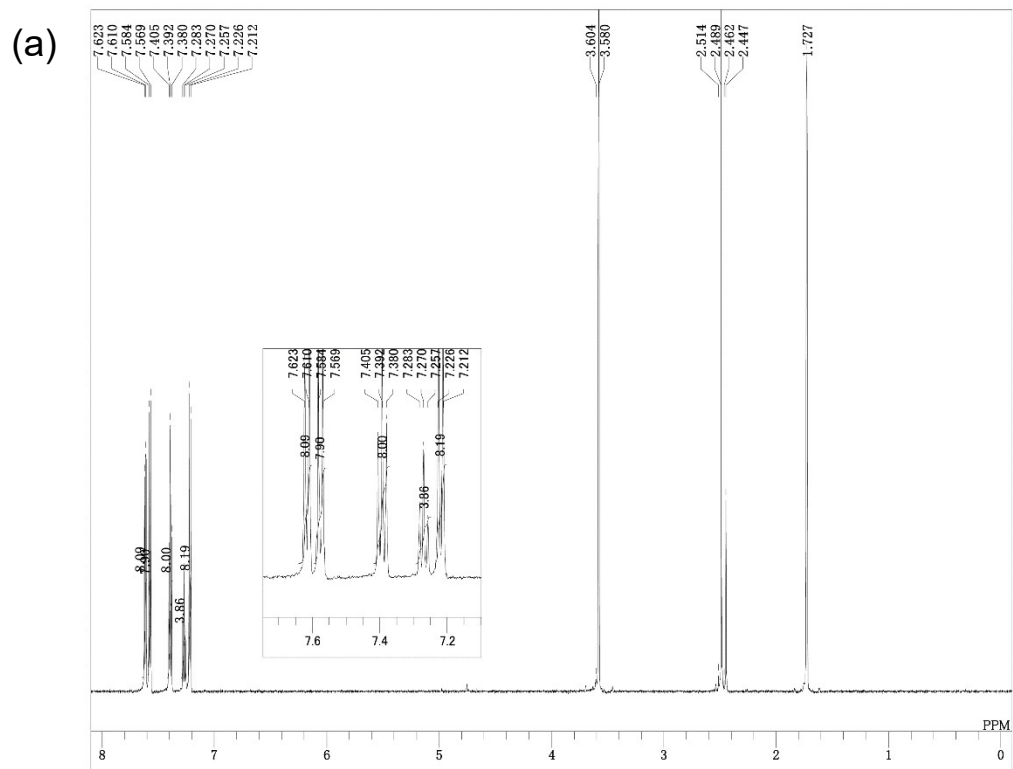


Fig. S12 ^1H -NMR spectra of (a) BPBPA-D1 and (b) D2.